INTERNATIONAL JOURNAL FOR NUMERICAL METHODS IN FLUIDS
Int. J. Numer. Meth. Fluids 2007; **53**:129–147
Published online 19 June 2006 in Wiley InterScience (www.interscience.wiley.com). DOI: 10.1002/fld.1252

A parametric finite-difference method for shallow sea waves

A. G. Bratsos[1,*,†], I. Th. Famelis[1,‡] and A. M. Prospathopoulos[2,§]

[1]*Department of Mathematics, Technological Educational Institution (T.E.I.) of Athens, GR 122 10 Egaleo, Athens, Greece*
[2]*Hellenic Center for Marine Research (HCMR), Institute of Oceanography, P.O. Box 712, GR-190 13 Anavyssos, Greece*

SUMMARY

This paper presents a parametric finite-difference scheme concerning the numerical solution of the one-dimensional Boussinesq-type set of equations, as they were introduced by Peregrine (*J. Fluid Mech.* 1967; **27**(4)) in the case of waves relatively long with small amplitudes in water of varying depth. The proposed method, which can be considered as a generalization of the Crank-Nickolson method, aims to investigate alternative approaches in order to improve the accuracy of analogous methods known from bibliography. The resulting linear finite-difference scheme, which is analysed for stability using the Fourier method, has been applied successfully to a problem used by Beji and Battjes (*Coastal Eng.* 1994; **23**: 1–16), giving numerical results which are in good agreement with the corresponding results given by MIKE 21 BW (User Guide. In: *MIKE 21*, *Wave Modelling*, *User Guide*. 2002; 271–392) developed by DHI Software. Copyright © 2006 John Wiley & Sons, Ltd.

Received 2 January 2005; Revised 10 April 2006; Accepted 11 April 2006

KEY WORDS: shallow water waves; Boussinesq equations; numerical modelling; finite-difference method

1. INTRODUCTION

During the last three decades a lot of effort has been put by the scientific community on numerical modelling of short waves in shallow water. Most of the phase-resolving models dealing with this research aspect and used in practical applications are based either on the mild-slope equation,

*Correspondence to: A. G. Bratsos, Department of Mathematics, Technological Educational Institution (T.E.I.) of Athens, GR 122 10 Egaleo, Athens, Greece.
†E-mail: bratsos@teiath.gr
‡E-mail: ifamelis@teiath.gr
§E-mail: aprosp@ath.hcmr.gr

Contract/grant sponsor: E.E.
Contract/grant sponsor: Greek Government

originally derived by Berkhoff [1], which describes the motion of time harmonic water waves of infinitesimal height (linear waves) on a gently sloping bathymetry with arbitrary water depth, or based on the Boussinesq-type equations governing the propagation of arbitrary long-wave disturbances of small to moderate amplitude over a slowly-varying bathymetry, the first such set of which was derived by Peregrine [2]. In case the research is interested in the energy transfer among the different components of shallow waves as those propagate from offshore inshore into shallow water, then Boussinesq-type equations—which are weakly non-linear and dispersive—have been found to model the non-linear effects of the wave-transformation process with satisfactory accuracy. These equations are depth integrated, simplifying the full three-dimensional problem to a two-dimensional one, and can be formulated either in the time-domain (most usual) or in the frequency domain.

Most of the works dealing with numerical modelling in the time-domain employ finite difference methods (FDM). Characteristic pioneer works on FDM concerning short-wave modelling in shallow water were those of Abbott *et al.* [3] according to which the differential equations were discretized by using a time-centred implicit scheme with variables defined on a space-staggered rectangular grid, as well as the one of Abbott *et al.* [4], including developments of the aforementioned scheme. Based on the same numerical method, Madsen *et al.* [5] presented a new form of equations in terms of the depth-integrated velocities for two horizontal dimensions with improved linear shallow and dispersion characteristics and Madsen and Sørensen [6] rederived the new Boussinesq equations for slowly varying bathymetry. Beji and Battjes [7] used similar equations and scheme to model relatively long, unidirectional waves propagating over a submerged obstacle. Wei and Kirby [8] developed a high-order numerical FDM scheme to solve a set of highly non-linear Boussinesq-type equations, while Beji and Nadaoka [9] used three-time-level finite-difference approximations to model the corrected (energy conserving) equations of Madsen and Sørensen [6]. For general, extended reviews on the Boussinesq-type modelling the reader can find resource in the works of Madsen and Schäffer [10] and Kirby [11].

In this paper a parametric numerical scheme based on a generalization of the Crank-Nickolson method is used to simulate weakly-non-linear wave propagation over variable bathymetry regions in shallow water conditions. The organization of the paper is as follows: in Section 2, the physical problem is set and its governing equations are stated. Next in Section 3, the numerical scheme and its stability analysis are presented. Finally in Section 4, the numerical results arising from the experiments using the proposed method are analysed and discussed.

2. GOVERNING EQUATIONS

Following Peregrine [2] the equations of motion describing relatively long, small amplitude waves propagating in water of varying depth in $2+1$ dimensions are given by

$$\frac{\partial \zeta}{\partial t} + \nabla \cdot [(h+\zeta)\mathbf{u}] = 0 \tag{1a}$$

$$\mathbf{u}_t + (\mathbf{u}\cdot\nabla)\mathbf{u} + g\nabla\zeta = \frac{1}{2}h\frac{\partial}{\partial t}\nabla[\nabla\cdot(h\mathbf{u})] - \frac{1}{6}h^2\frac{\partial}{\partial t}\nabla(\nabla\cdot\mathbf{u}) \tag{1b}$$

in the region $\tilde{\Omega} = \{(x, y);\ L_x^0 < x < L_x^1,\ L_y^0 < y < L_y^1\}$ for $t > 0$ where $\zeta = \zeta(x, y, t)$ is the free surface displacement as it is measured from still water level and $\mathbf{u} = \mathbf{u}(x, y, t) = [u_1, u_2]^{\mathrm{T}}$ T denoting

DOI: 10.1002/fld

transpose, is the depth-averaged horizontal velocity vector both sufficient differentiable functions, $\nabla = [\partial/\partial x, \partial/\partial y]^{\mathrm{T}}$, $h = h(x, y)$ is the still water depth and g the gravitational acceleration.

Systems (1a) and (1b) for the one-dimensional propagation, when $\partial^2 h/\partial x^2 = 0$ (see Reference [7]), $h = h(x)$ and it is set for simplicity $u_1 \equiv u$, reads to

$$\frac{\partial \zeta}{\partial t} + \frac{\partial[(h+\zeta)u]}{\partial x} = 0 \tag{2a}$$

$$\frac{\partial u}{\partial t} + u\frac{\partial u}{\partial x} + g\frac{\partial \zeta}{\partial x} = \frac{1}{3}h^2\frac{\partial^3 u}{\partial x^2 \partial t} + h\frac{\partial h}{\partial x}\frac{\partial^2 u}{\partial x \partial t} \tag{2b}$$

where it is assumed that $x \in \Omega$ with $\Omega = [L_0 < x < L_1]$ and $t > 0$. Madsen *et al.* [5] have given a formulation for horizontal bottom by adding in Equation (2b) a third-order derivative term with an adjustable proportional factor, which is known as the *calibration* factor b, as follows:

$$\frac{\partial u}{\partial t} + u\frac{\partial u}{\partial x} + g\frac{\partial \zeta}{\partial x} = \frac{1}{3}h^2\frac{\partial^3 u}{\partial x^2 \partial t} + h\frac{\partial h}{\partial x}\frac{\partial^2 u}{\partial x \partial t} + bh^2\left(\frac{\partial^3 u}{\partial x^2 \partial t} + g\frac{\partial^3 \zeta}{\partial x^3}\right)$$

Then systems (2a) and (2b) is written as

$$\frac{\partial \zeta}{\partial t} + \frac{\partial[(h+\zeta)u]}{\partial x} = 0 \tag{3a}$$

$$\frac{\partial u}{\partial t} + u\frac{\partial u}{\partial x} + g\frac{\partial \zeta}{\partial x} = \tilde{b}h^2\frac{\partial^3 u}{\partial x^2 \partial t} + h\frac{\partial h}{\partial x}\frac{\partial^2 u}{\partial x \partial t} + gbh^2\frac{\partial^3 \zeta}{\partial x^3} \tag{3b}$$

in which $\tilde{b} = b + \frac{1}{3}$. Appropriate values for b could be found in References [6, 7], etc.

The initial conditions associated with systems (3a) and (3b) have been assumed to be of the form

$$u(x, 0) = \zeta(x, 0) = 0 \tag{4}$$

3. THE NUMERICAL SCHEME

3.1. Grid and solution vectors

To obtain a numerical solution the region $R = \Omega \times [t > 0]$ with its boundary ∂R consisting of the lines $x = L_0$, L_1 and $t = 0$ is covered with a rectangular mesh, G, of points with coordinates $(x, t) = (x_m, t_n) = (L_0 + m\Delta x, n\Delta t)$ with $m = 0, 1, \ldots, N+1$ and $n = 0, 1, \ldots,$ in which $\Delta x = (L_1 - L_0)/(N+1)$ represents the discretization into $N+1$ subintervals of the space variable x, while Δt represents the discretization of the time variable t. The solution for the unknown functions ζ and u of an approximating finite-difference scheme at the same point will be denoted by ζ_m^n and u_m^n, respectively, while for the purpose of analysing stability, the numerical value of actually obtained (subject, for instance, to computer round-off errors) will be denoted by $\tilde{\zeta}_m^n$ and $\tilde{u}_m^n$.

DOI: 10.1002/fld

Let the solution vectors be

$$\boldsymbol{\zeta}^n = \boldsymbol{\zeta}(t_n) = [\zeta_1^n, \zeta_2^n, \ldots, \zeta_N^n, \zeta_{N+1}^n]^{\mathrm{T}} \tag{5a}$$

$$\mathbf{u}^n = \mathbf{u}(t_n) = [u_1^n, u_2^n, \ldots, u_N^n, u_{N+1}^n]^{\mathrm{T}} \tag{5b}$$

For the finite-difference scheme the following formulae are going to be used:

$$\frac{\partial u}{\partial t} \approx \frac{u(x, t+\Delta t) - u(x,t)}{\Delta t} = \frac{1}{\Delta t}(u_m^{n+1} - u_m^n) \tag{6}$$

$$\frac{\partial u}{\partial x} \approx \frac{u(x+\Delta x, t) - u(x-\Delta x, t)}{2\Delta x} = \frac{1}{2\Delta x}(u_{m+1}^n - u_{m-1}^n) \tag{7a}$$

while, when $m = 1$ or $m = N+1$:

$$\frac{\partial u}{\partial x} \approx \frac{u(x+\Delta x, t) - u(x,t)}{\Delta x} = \frac{1}{\Delta x}(u_{m+1}^n - u_m^n) \tag{7b}$$

or

$$\frac{\partial u}{\partial x} \approx \frac{u(x,t) - u(x-\Delta x, t)}{\Delta x} = \frac{1}{\Delta x}(u_m^n - u_{m-1}^n) \tag{7c}$$

Also

$$\frac{\partial^2 u}{\partial x^2} \approx \frac{u(x+\Delta x, t) - 2u(x,t) + u(x-\Delta x, t)}{\Delta x^2} = \frac{1}{\Delta x^2}(u_{m+1}^n - 2u_m^n + u_{m-1}^n) \tag{8}$$

$$\begin{aligned}\frac{\partial^2 u}{\partial x \partial t} &\approx \frac{1}{2\Delta x \Delta t}[u(x+\Delta x, t+\Delta t) - u(x-\Delta x, t+\Delta t) - u(x+\Delta x, t) + u(x-\Delta x, t)] \\ &= \frac{1}{2\Delta x \Delta t}(u_{m+1}^{n+1} - u_{m-1}^{n+1} - u_{m+1}^n + u_{m-1}^n)\end{aligned} \tag{9}$$

$$\begin{aligned}\frac{\partial^3 u}{\partial x^3} &\approx \frac{-u(x-2\Delta x, t) + 2u(x-\Delta x, t) - 2u(x+\Delta x, t) + u(x+2\Delta x, t)}{2\Delta x^3} \\ &= \frac{1}{2\Delta x^3}(-u_{m-2}^n + 2u_{m-1}^n - 2u_{m+1}^n + u_{m+2}^n)\end{aligned} \tag{10}$$

$$\begin{aligned}\frac{\partial^3 u}{\partial x^2 \partial t} &\approx \frac{1}{\Delta x^2 \Delta t}[u(x+\Delta x, t+\Delta t) - 2u(x, t+\Delta t) + u(x-\Delta x, t+\Delta t) \\ &\quad - u(x+\Delta x, t) + 2u(x,t) - u(x-\Delta x, t)] \\ &= \frac{1}{\Delta x^2 \Delta t}(u_{m+1}^{n+1} - 2u_m^{n+1} + u_{m-1}^{n+1} - u_{m+1}^n + 2u_m^n - u_{m-1}^n)\end{aligned} \tag{11}$$

DOI: 10.1002/fld

3.2. The proposed method

Using an analogous scheme as in Reference [12] the systems (3a) and (3b) is considered to be satisfied at the point $(m\Delta x, (n+\vartheta)\Delta t)$; $\vartheta \in [0, 1]$ of the grid G. Due to this assumption all space partial derivatives are substituted by their finite-difference approximations at the nth and $(n+1)$th time-level. This method for $\partial u/\partial x$ using Equation (7a) gives

$$\left(\frac{\partial u}{\partial x}\right)_m^{n+\vartheta} = \vartheta\left(\frac{\partial u}{\partial x}\right)_m^{n+1} + (1-\vartheta)\left(\frac{\partial u}{\partial x}\right)_m^{n}$$

$$= \frac{1}{2\Delta x}[\vartheta(u_{m+1}^{n+1} - u_{m-1}^{n+1}) + (1-\vartheta)(u_{m+1}^{n} - u_{m-1}^{n})] \tag{12}$$

while for $\partial^3 u/\partial x^3$ using Equation (10)

$$\left(\frac{\partial^3 u}{\partial x^3}\right)_m^{n+\vartheta} = \vartheta\left(\frac{\partial^3 u}{\partial x^3}\right)_m^{n+1} + (1-\vartheta)\left(\frac{\partial^3 u}{\partial x^3}\right)_m^{n} = \frac{1}{2\Delta x^3}[\vartheta(-u_{m-2}^{n+1} + 2u_{m-1}^{n+1}$$

$$- 2u_{m+1}^{n+1} + u_{m+2}^{n+1}) + (1-\vartheta)(-u_{m-2}^{n} + 2u_{m-1}^{n} - 2u_{m+1}^{n} + u_{m+2}^{n})] \tag{13}$$

Equations (12) and (13), when $\vartheta = \frac{1}{2}$, lead to the Crank-Nickolson scheme used by Beji and Battjes [7].

3.2.1. The boundary conditions. The surface elevation is specified at the boundary point $x = L_0$ (*input*) as

$$\zeta(L_0, t) = f(t), \quad t > 0 \tag{14a}$$

where $f(t)$ is an appropriate function producing harmonic waves of period T and height H, while at the same point the depth-averaged velocity using the continuity equation for a progressive wave as

$$u(L_0, t) = \frac{\tilde{c}_0 \zeta(L_0, t)}{h_0 + \zeta(L_0, t)}, \quad t > 0 \tag{14b}$$

where $\tilde{c}_0$ and h_0 are the phase celerity and the water depth at $x = L_0$, respectively. The phase celerity is computed from the linear dispersion relation corresponding to Equations (3a) and (3b) from the (dominant) incident wave period. Equations (14a) and (14b) using the notation of the grid G are written as

$$\zeta_0^n = f(n\Delta t) \tag{15a}$$

and

$$u_0^n = \frac{\tilde{c}_0 \zeta_0^n}{h_0 + \zeta_0^n} \tag{15b}$$

DOI: 10.1002/fld

At the outgoing boundary (*output*) $x = L_1$ the values $\zeta(L_1, t)$ and $u(L_1, t)$ are evaluated from the radiation condition for both the surface displacement using the continuity equation and for the velocity from the momentum one defined by

$$\frac{\partial \zeta(L_1,t)}{\partial t} + \tilde{c}_{N+1} \left.\frac{\partial \zeta(x,t)}{\partial x}\right|_{x=L_1} = 0, \quad t>0 \tag{16a}$$

$$\frac{\partial u(L_1,t)}{\partial t} + \tilde{c}_{N+1} \left.\frac{\partial u(x,t)}{\partial x}\right|_{x=L_1} = 0, \quad t>0 \tag{16b}$$

where $\tilde{c}_{N+1}$ and h_{N+1} are the phase celerity and the water depth at $x = L_1$. Equations (16a) and (16b) using the proposed method (12) for both the time and the space partial derivatives give

$$\vartheta \left(\frac{\partial \zeta}{\partial t}\right)_{N+1}^{n+1} + (1-\vartheta)\left(\frac{\partial \zeta}{\partial t}\right)_{N}^{n+1} = -\tilde{c}_{N+1}\left[\vartheta\left(\frac{\partial \zeta}{\partial x}\right)_{N+1}^{n+1} + (1-\vartheta)\left(\frac{\partial \zeta}{\partial x}\right)_{N+1}^{n}\right]$$

$$\vartheta \left(\frac{\partial u}{\partial t}\right)_{N+1}^{n+1} + (1-\vartheta)\left(\frac{\partial u}{\partial t}\right)_{N}^{n+1} = -\tilde{c}_{N+1}\left[\vartheta\left(\frac{\partial u}{\partial x}\right)_{N+1}^{n+1} + (1-\vartheta)\left(\frac{\partial u}{\partial x}\right)_{N+1}^{n}\right]$$

or using Equation (6) for the time and Equation (7c) for the space partial derivatives and the notation of the grid G:

$$\begin{aligned}&\vartheta(\zeta_{N+1}^{n+1} - \zeta_{N+1}^{n}) + (1-\vartheta)(\zeta_{N}^{n+1} - \zeta_{N}^{n}) \\ &\quad = -r\tilde{c}_{N+1}[\vartheta(\zeta_{N+1}^{n+1} - \zeta_{N}^{n+1}) + (1-\vartheta)(\zeta_{N+1}^{n} - \zeta_{N}^{n})]\end{aligned} \tag{17a}$$

$$\begin{aligned}&\vartheta(u_{N+1}^{n+1} - u_{N+1}^{n}) + (1-\vartheta)(u_{N}^{n+1} - u_{N}^{n}) \\ &\quad = -r\tilde{c}_{N+1}[\vartheta(u_{N+1}^{n+1} - u_{N}^{n+1}) + (1-\vartheta)(u_{N+1}^{n} - u_{N}^{n})]\end{aligned} \tag{17b}$$

in which $r = \Delta t/\Delta x$, otherwise

$$\begin{aligned}&\vartheta(1 + r\tilde{c}_{N+1})\zeta_{N+1}^{n+1} + [1 - \vartheta(1 + r\tilde{c}_{N+1})]\zeta_{N}^{n+1} \\ &\quad = [\vartheta - r\tilde{c}_{N+1}(1-\vartheta)]\zeta_{N+1}^{n} + (1-\vartheta)(1 + r\tilde{c}_{N+1})\zeta_{N}^{n}\end{aligned} \tag{18a}$$

$$\begin{aligned}&\vartheta(1 + r\tilde{c}_{N+1})u_{N+1}^{n+1} + [1 - \vartheta(1 + r\tilde{c}_{N+1})]u_{N}^{n+1} \\ &\quad = [\vartheta - r\tilde{c}_{N+1}(1-\vartheta)]u_{N+1}^{n} + (1-\vartheta)(1 + r\,\tilde{c}_{N+1})u_{N}^{n}\end{aligned} \tag{18b}$$

with $\vartheta \in (0, 1]$. Especially, when $\vartheta = 0$, the following approximations arising by Equations (16a) and (16b) are going to be used:

$$\zeta_{N+1}^{n+1} = \zeta_{N+1}^{n} - r\tilde{c}_{N+1}(\zeta_{N+1}^{n} - \zeta_{N}^{n}) \tag{19a}$$

$$u_{N+1}^{n+1} = u_{N+1}^{n} - r\tilde{c}_{N+1}(u_{N+1}^{n} - u_{N}^{n}) \tag{19b}$$

DOI: 10.1002/fld

Finally, after using linear interpolation the following approximations for the first out of the boundary points of the grid G were used:

$$\zeta(L_0-\Delta x,t)\approx 2\zeta(L_0,t)-\zeta(L_0+\Delta x,t),\quad t>0$$

$$\zeta(L_1+\Delta x,t)\approx 2\zeta(L_1,t)-\zeta(L_1-\Delta x,t),\quad t>0$$

otherwise, using the notation of the grid G,

$$\zeta_{-1}^n=2\zeta_0^n-\zeta_1^n \tag{20a}$$

$$\zeta_{N+2}^n=2\zeta_{N+1}^n-\zeta_N^n \tag{20b}$$

3.2.2. The finite-difference scheme. Let $p=1/\Delta x^2$ and $q=bg\Delta t/4\Delta x^3$. Then Equation (3a) using Equations (6)–(7c) leads to the following two-time level *explicit* finite-difference scheme for the evaluation of the unknown vector $\boldsymbol{\zeta}^{n+1}$:

$$\zeta_m^{n+1}=\zeta_m^n-\frac{r}{2}[(h_{m+1}+\zeta_{m+1}^n)u_{m+1}^n-(h_{m-1}+\zeta_{m-1}^n)u_{m-1}^n] \tag{21a}$$

for $m=1,2,\ldots,N$,

$$\begin{aligned}\zeta_{N+1}^{n+1}=\frac{1}{\vartheta(1+r\tilde{c}_{N+1})}\{&-[1-\vartheta(1+r\tilde{c}_{N+1})]\zeta_N^{n+1}\\&+[\vartheta-r\tilde{c}_{N+1}(1-\vartheta)]\zeta_{N+1}^n+(1-\vartheta)(1+r\tilde{c}_{N+1})\zeta_N^n\}\quad\text{when }\vartheta\in(0,1]\end{aligned} \tag{21b}$$

using Equation (18a) or using Equation (19a)

$$\zeta_{N+1}^{n+1}=\zeta_{N+1}^n-r\tilde{c}_{N+1}(\zeta_{N+1}^n-\zeta_N^n)\quad\text{when }\vartheta=0 \tag{21c}$$

Equation (3b), subject to the boundary conditions specified in Section 3.2.1, forms the following two-time level *implicit* finite-difference scheme for the unknown vector $\mathbf{u}^{n+1}$:

$$\begin{aligned}&\left[\frac{r}{2}\vartheta u_1^{n+\vartheta}-\tilde{b}h_1^2p-\frac{1}{4}ph_1(h_2-h_0)\right]u_2^{n+1}+(1+2\tilde{b}h_1^2p)u_1^{n+1}\\&=-\left[-\frac{r}{2}\vartheta u_1^{n+\vartheta}-\tilde{b}h_1^2p+\frac{1}{4}ph_1(h_2-h_0)\right]u_0^{n+1}\\&\quad+\left[-\frac{r}{2}(1-\vartheta)u_1^{n+\vartheta}-\tilde{b}h_1^2p-\frac{1}{4}ph_1(h_2-h_0)\right]u_2^n\\&\quad+(1+2\tilde{b}h_1^2p)u_1^n+\left[\frac{r}{2}(1-\vartheta)u_1^{n+\vartheta}-\tilde{b}h_1^2p+\frac{1}{4}ph_1(h_2-h_0)\right]u_0^n\\&\quad+2qh_1^2[\vartheta(\zeta_3^{n+1}+\zeta_1^{n+1}-2\zeta_0^{n+1})+(1-\vartheta)(\zeta_3^n+\zeta_1^n-2\zeta_0^n)]\\&\quad-\left(4qh_1^2+\frac{r}{2}g\right)[\vartheta(\zeta_2^{n+1}-\zeta_0^{n+1})+(1-\vartheta)(\zeta_2^n-\zeta_0^n)]\end{aligned} \tag{22a}$$

DOI: 10.1002/fld

for $m=1$,

$$\left[\frac{r}{2}\vartheta u_m^{n+\vartheta}-\tilde{b}h_m^2 p-\frac{1}{4}ph_m(h_{m+1}-h_{m-1})\right]u_{m+1}^{n+1}$$

$$+(1+2\tilde{b}h_m^2 p)u_m^{n+1}+\left[-\frac{r}{2}\vartheta u_m^{n+\vartheta}-\tilde{b}h_m^2 p+\frac{1}{4}ph_m(h_{m+1}-h_{m-1})\right]u_{m-1}^{n+1}$$

$$=\left[-\frac{r}{2}(1-\vartheta)u_m^{n+\vartheta}-\tilde{b}h_m^2 p-\frac{1}{4}ph_m(h_{m+1}-h_{m-1})\right]u_{m+1}^{n}$$

$$+(1+2\tilde{b}h_m^2 p)u_m^{n}+\left[\frac{r}{2}(1-\vartheta)u_m^{n+\vartheta}-\tilde{b}h_m^2 p+\frac{1}{4}ph_m(h_{m+1}-h_{m-1})\right]u_{m-1}^{n}$$

$$+2qh_m^2[\vartheta(\zeta_{m+2}^{n+1}-\zeta_{m-2}^{n+1})+(1-\vartheta)(\zeta_{m+2}^{n}-\zeta_{m-2}^{n})]$$

$$-(4qh_m^2+\frac{r}{2}g)[\vartheta(\zeta_{m+1}^{n+1}-\zeta_{m-1}^{n+1})+(1-\vartheta)(\zeta_{m+1}^{n}-\zeta_{m-1}^{n})] \tag{22b}$$

for $m=2,3,\ldots,N-1$,

$$\left[\frac{r}{2}\vartheta u_N^{n+\vartheta}-\tilde{b}h_N^2 p-\frac{1}{4}ph_N(h_{N+1}-h_{N-1})\right]u_{N+1}^{n+1}$$

$$+(1+2\tilde{b}h_N^2 p)u_N^{n+1}+\left[-\frac{r}{2}\vartheta u_N^{n+\vartheta}-\tilde{b}h_N^2 p+\frac{1}{4}ph_N(h_{N+1}-h_{N-1})\right]u_{N-1}^{n+1}$$

$$=\left[-\frac{r}{2}(1-\vartheta)u_N^{n+\vartheta}-\tilde{b}h_N^2 p-\frac{1}{4}h_N p(h_{N+1}-h_{N-1})\right]u_{N+1}^{n}$$

$$+(1+2\tilde{b}h_N^2 p)u_N^{n}+\left[\frac{r}{2}(1-\vartheta)u_N^{n+\vartheta}-\tilde{b}h_N^2 p+\frac{1}{4}ph_N(h_{N+1}-h_{N-1})\right]u_{N-1}^{n}$$

$$+2qh_N^2[\vartheta(2\zeta_{N+1}^{n+1}-\zeta_N^{n+1}-\zeta_{N-2}^{n+1}))+(1-\vartheta)(2\zeta_{N+1}^{n}-\zeta_N^{n}-\zeta_{N-2}^{n})]$$

$$-(4qh_N^2+\frac{r}{2}g)[\vartheta(\zeta_{N+1}^{n+1}-\zeta_{N-1}^{n+1})+(1-\vartheta)(\zeta_{N+1}^{n}-\zeta_{N-1}^{n})] \tag{22c}$$

for $m=N$,

$$\vartheta(1+r\tilde{c}_{N+1})u_{N+1}^{n+1}+[1-\vartheta(1+r\tilde{c}_{N+1})]u_N^{n+1}$$

$$=[\vartheta-r\tilde{c}_{N+1}(1-\vartheta)]u_{N+1}^{n}+(1-\vartheta)(1+r\tilde{c}_{N+1})u_N^{n}\quad\text{when } \vartheta\in(0,1] \tag{22d}$$

DOI: 10.1002/fld

using Equation (18b) or from Equation (19b)

$$u_{N+1}^{n+1} = u_{N+1}^{n} - r\tilde{c}_{N+1}(u_{N+1}^{n} - u_{N}^{n}) \quad \text{when } \vartheta = 0 \tag{22e}$$

The term $u_m^{n+\vartheta}$; $m = 1, 2, \ldots, N$, in Equations (22a)–(22c) is determined using Taylor's series expansion about (x, t) as follows:

$$u(x, t + \vartheta\Delta t) = u(x, t) + \vartheta\Delta t \frac{\partial u(x, t)}{\partial t} + O(\Delta t^2) \quad \text{as } \Delta t \to 0 \tag{23}$$

In Equation (23) the term $\partial u/\partial t$ can be evaluated explicitly by employing the momentum equation for the shallow water approximation as follows:

$$\frac{\partial u}{\partial t} + u\frac{\partial u}{\partial x} + g\frac{\partial \zeta}{\partial x} \approx 0 \tag{24}$$

Then using the notation of the grid G and Equations (7a)–(7c), (23) and (24) give

$$u_m^{n+\vartheta} = u_m^n - \frac{r}{2}\vartheta[u_m^n(u_{m+1}^n - u_{m-1}^n) + g(\zeta_{m+1}^n - \zeta_{m-1}^n)] \tag{25}$$

for $m = 1, 2, \ldots, N$.

Finally Equations (22a)–(22e) are written in a matrix–vector form as

$$\tilde{A}\mathbf{u}^{n+1} = \mathbf{F}(\mathbf{u}^n, \boldsymbol{\zeta}^{n+1}, \boldsymbol{\zeta}^n) + \mathbf{b}_d \tag{26}$$

in which $\tilde{A}$ is a tridiagonal matrix of order $N + 1$ given by

$$\tilde{A} = \begin{bmatrix} d_1 & e_1 & & & & \\ c_2 & d_2 & e_2 & & & \\ & & . & . & . & \\ & & & c_N & d_N & e_N \\ & & & & c_{N+1} & d_{N+1} \end{bmatrix} \tag{27}$$

with entries defined in Equations (22a)–(22e) and

$$\mathbf{b}_d = \left[-\left\{ -\frac{r}{2}\vartheta u_1^{n+\vartheta} - \tilde{b}h_1^2 p + \frac{1}{4}ph_1(h_2 - h_0) \right\} u_0^{n+1}, 0, \ldots, 0 \right]^{\mathrm{T}} \tag{28}$$

the vector with the boundary conditions of order $N + 1$.

Then the values ζ_m^{n+1}; $m = 1, 2, \ldots, N$, evaluated by Equations (21a)–(21c), are *corrected* using the values of $\mathbf{u}^{n+1}$ obtained from the solution of the system Equation (26) with an analogous scheme to that used in Equation (12)

$$\begin{aligned} \zeta_m^{n+1} = \zeta_m^n - \frac{r}{2}\{&\vartheta[(h_{m+1} + \zeta_{m+1}^{n+1})u_{m+1}^{n+1} - (h_{m-1} + \zeta_{m-1}^{n+1})u_{m-1}^{n+1}] \\ &+ (1 - \vartheta)[(h_{m+1} + \zeta_{m+1}^n)u_{m+1}^n - (h_{m-1} + \zeta_{m-1}^n)u_{m-1}^n]\} \end{aligned} \tag{29}$$

DOI: 10.1002/fld

for $m = 1, 2, \ldots, N$. The above procedure can be described as follows:

(i) **P**: predict the value $\boldsymbol{\zeta}^{n+1}$ from Equations (21a)–(21c),
(ii) **E**: evaluate the value $\mathbf{u}^{n+1}$ from Equation (27),
(iii) **C**: correct $\boldsymbol{\zeta}^{n+1}$ using Equation (29),

repeat the above steps (ii)–(iii) to achieve the desired accuracy.

3.3. Stability analysis

The von Neumann method of analysing stability will be used. This method entails considering a small error of the form

$$Z_m^n = \zeta_m^n - \tilde{\zeta}_m^n = \mathrm{e}^{n\alpha\Delta t}\mathrm{e}^{\mathrm{i}m\beta_\zeta \Delta x} \tag{30a}$$

$$\hat{Z}_m^n = u_m^n - \tilde{u}_m^n = \mathrm{e}^{n\alpha\Delta t}\mathrm{e}^{\mathrm{i}m\beta_u \Delta x} \quad \text{with } i = \sqrt{-1};\ \alpha \in \mathscr{C},\ \beta_\zeta, \beta_u \in \Re \tag{30b}$$

and then finding the criteria under which the von Neumann necessary criterion for stability

$$|\mathrm{e}^{\alpha\Delta t}| \leqslant 1 \tag{31}$$

where $\mathrm{e}^{\alpha\Delta t}$ is the amplification factor, is satisfied.

Let

$$h_0 \text{ be a constant typical value of } h_m;\ m = 0, 1, \ldots, N+1 \tag{32a}$$

$$\tilde{\zeta}_0 = \max_{m=0,1,\ldots,N+1}(h_m + \zeta_m^n) \tag{32b}$$

$$u_0 = \max_{m=0,1,\ldots,N+1} u_m^n \tag{32c}$$

and

$$\tilde{u}_0 = \max_{m=0,1,\ldots,N+1} u_m^{n+\vartheta} \tag{32d}$$

Equation (21a) using the linearization (32c) is written as

$$\zeta_m^{n+1} - \zeta_m^n + \frac{r}{2}u_0(h_{m+1} + \zeta_{m+1}^n - h_{m-1}^n - \zeta_{m-1}^n) = 0$$

which using (30a) and (32a) gives rise to the following scheme for examining stability:

$$Z_m^{n+1} - Z_m^n + \frac{r}{2}u_0(Z_{m+1}^n - Z_{m-1}^n) = 0 \tag{33}$$

Equation (33) using expression (30a) after canceling both sides with $\mathrm{e}^{n\alpha\Delta t}\,\mathrm{e}^{\mathrm{i}m\beta_\zeta\Delta x}$, leads to the following stability equation

$$\mathrm{e}^{\alpha\Delta t} + \mathrm{i}ru_0 \sin(\beta_\zeta \Delta x) - 1 = 0 \tag{34}$$

Then condition (31) for Equation (34) using known properties of the modulus gives the following condition:

$$|\mathrm{e}^{\alpha\Delta t}| \leqslant 1 + u_0\frac{\Delta t}{\Delta x} \tag{35}$$

DOI: 10.1002/fld

which is always satisfied, when

$$u_0 = 0 \tag{36}$$

If $u_0 = \max u_m^0;\ m = 1, 2, \ldots, N+1$ condition (36) is in accordance with the initial condition (4). Also condition (36) satisfies the CFL condition [13] for first-order hyperbolic equations (see Reference [14]) according to which

$$u_0 \frac{\Delta t}{\Delta x} \leqslant 1 \tag{37}$$

Equation (21a) using linearization (32b) is written as

$$\zeta_m^{n+1} - \zeta_m^n = -\frac{r}{2}\tilde{\zeta}_0 (u_{m+1}^n - u_{m-1}^n) \tag{38}$$

Then Equation (22b) using linearizations (32a)–(32d) reads to

$$\begin{aligned}
&\frac{r}{2}\vartheta\tilde{u}_0(u_{m+1}^{n+1} - u_{m-1}^{n+1}) - \tilde{b}h_0^2 p(u_{m+1}^{n+1} - 2u_m^{n+1} + u_{m-1}^{n+1}) + u_m^{n+1} \\
&\quad = -\frac{r}{2}(1-\vartheta)\tilde{u}_0(u_{m+1}^n - u_{m-1}^n) - \tilde{b}h_0^2 p(u_{m+1}^n - 2u_m^n + u_{m-1}^n) + u_m^n \\
&\qquad + 2qh_0^2[\vartheta(\zeta_{m+2}^{n+1} - \zeta_{m+2}^n) - \vartheta(\zeta_{m-2}^{n+1} - \zeta_{m-2}^n) + (\zeta_{m+2}^n - \zeta_{m-2}^n)] \\
&\qquad - (4q\,h_0^2 + \frac{r}{2}g)[\vartheta(\zeta_{m+1}^{n+1} - \zeta_{m+1}^n) - \vartheta(\zeta_{m-1}^{n+1} - \zeta_{m-1}^n) + (\zeta_{m+1}^n - \zeta_{m-1}^n)]
\end{aligned}$$

otherwise using Equation (38) as

$$\begin{aligned}
&\frac{r}{2}\vartheta\tilde{u}_0(u_{m+1}^{n+1} - u_{m-1}^{n+1}) - \tilde{b}h_0^2 p(u_{m+1}^{n+1} - 2u_m^{n+1} + u_{m-1}^{n+1}) + u_m^{n+1} \\
&\quad = -\frac{r}{2}(1-\vartheta)\tilde{u}_0(u_{m+1}^n - u_{m-1}^n) - \tilde{b}h_0^2 p(u_{m+1}^n - 2u_m^n + u_{m-1}^n) + u_m^n \\
&\qquad + qrh_0^2\tilde{\zeta}_0\vartheta(-u_{m+3}^n + u_{m+1}^n + u_{m-1}^n - u_{m-3}^n) \\
&\qquad + \frac{r}{2}\tilde{\zeta}_0\vartheta\left(4qh_0^2 + \frac{r}{2}g\right)(u_{m+2}^n - 2u_m^n + u_{m-2}^n) \\
&\qquad + 2qh_0^2(\zeta_{m+2}^n - \zeta_{m-2}^n) - (4qh_0^2 + \frac{r}{2}g)(\zeta_{m+1}^n - \zeta_{m-1}^n)
\end{aligned} \tag{39}$$

To approximate the last two terms on the right-hand side of Equation (39) the approximation (24) by omitting the term $u(\partial u/\partial x)$ was used. Then

$$\zeta_{m+1}^n - \zeta_{m-1}^n = -\frac{2}{g}\frac{\Delta x}{\Delta t}(u_m^{n+1} - u_m^n) \tag{40a}$$

DOI: 10.1002/fld

and

$$\zeta_{m+2}^{n} - \zeta_{m-2}^{n} = -\frac{4}{g}\frac{\Delta x}{\Delta t}(u_m^{n+1} - u_m^n) \tag{40b}$$

Equation (39) using Equations (40a), (40b) and (30b) finally gives

$$\begin{aligned}
&\frac{r}{2}\vartheta\tilde{u}_0(\hat{Z}_{m+1}^{n+1} - \hat{Z}_{m-1}^{n+1}) - \tilde{b}h_0^2 p(\hat{Z}_{m+1}^{n+1} - 2\hat{Z}_m^{n+1} + \hat{Z}_{m-1}^{n+1}) \\
&\quad = -\frac{r}{2}(1-\vartheta)\tilde{u}_0(\hat{Z}_{m+1}^{n} - \hat{Z}_{m-1}^{n}) - \tilde{b}h_0^2 p(\hat{Z}_{m+1}^{n} - 2\hat{Z}_m^{n} + \hat{Z}_{m-1}^{n}) \\
&\qquad + qrh_0^2\tilde{\zeta}_0\vartheta(-\hat{Z}_{m+3}^{n} + \hat{Z}_{m+1}^{n} + \hat{Z}_{m-1}^{n} - \hat{Z}_{m-3}^{n}) \\
&\qquad + \frac{r}{2}\tilde{\zeta}_0\vartheta\left(4qh_0^2 + \frac{r}{2}g\right)(\hat{Z}_{m+2}^{n} - 2\hat{Z}_m^{n} + \hat{Z}_{m-2}^{n})
\end{aligned} \tag{41}$$

which after canceling both sides by $e^{n\alpha\Delta t}e^{im\beta_u\Delta x}$ leads to the following stability equation:

$$\begin{aligned}
&\left[ir\vartheta\tilde{u}_0\sin(\beta_u\Delta x) + 4\tilde{b}h_0^2 p\,\sin^2\left(\frac{\beta_u\Delta x}{2}\right)\right]\xi \\
&\quad = -ir(1-\vartheta)\tilde{u}_0\,\sin(\beta_u\Delta x) + 4\tilde{b}h_0^2 p\,\sin^2\left(\frac{\beta_u\Delta x}{2}\right) \\
&\qquad + 2qrh_0^2\tilde{\zeta}_0\vartheta[\cos(\beta_u\Delta x) - \cos(3\beta_u\Delta x)] - 2r\tilde{\zeta}_0\vartheta\left(4qh_0^2 + \frac{r}{2}g\right)\sin^2(\beta_u\Delta x)
\end{aligned} \tag{42}$$

where, again, $\xi = e^{\alpha\Delta t}$ the amplification factor. Equation (42) is of the form $\breve{A}\xi = \breve{B}$ with $\breve{A}$, $\breve{B} \in \mathscr{C}$, where $\mathscr{C}$ is the set of the complex numbers and $\breve{A} \neq 0$. Then $\xi = \breve{B}/\breve{A}$, so condition (31) will be satisfied, when

$$\left|\frac{\breve{B}}{\breve{A}}\right| \leqslant 1 \tag{43}$$

Ineq. (43), after applying known properties of the complex numbers, leads to

$$\begin{aligned}
&8g\vartheta\tilde{\zeta}_0\,\sin^2\left(\frac{\beta_u\Delta x}{2}\right)\left[1 + 4bph_0^2\,\sin^2\left(\frac{\beta_u\Delta x}{2}\right)\right]\left\{gr^2\vartheta\tilde{\zeta}_0\left[\cos^2\left(\frac{\beta_u\Delta x}{2}\right)\right.\right. \\
&\left.\left. + bph_0^2\,\sin^2(\beta_u\Delta x)\right] - 2\tilde{b}ph_0^2\right\} \leqslant (2\vartheta - 1)\tilde{u}_0^2
\end{aligned} \tag{44}$$

Let $\kappa = bph_0^2$, $\mu = \tilde{b}ph_0^2$. If $\vartheta > 0.5$, then Ineq. (44) gives the following restriction for r:

$$\left[\frac{2\mu}{g\vartheta\tilde{\zeta}_0(1+\kappa)}\right]^{1/2} < r \leqslant \left\{\left[g\vartheta\tilde{\zeta}_0(1+\kappa)\right]^{-1}\left[\frac{(2\vartheta-1)\tilde{u}_0^2}{8g\vartheta\tilde{\zeta}_0(1+4\kappa)} + 2\mu\right]\right\}^{1/2} \tag{45}$$

DOI: 10.1002/fld

If $\vartheta = 0.5$, then

$$r \leqslant 2\left[\frac{\mu}{g\tilde{\zeta}_0(1+\kappa)}\right]^{1/2} \tag{46}$$

and finally, when $\vartheta < 0.5$,

$$\left\{[g\vartheta\tilde{\zeta}_0(1+\kappa)]^{-1}\left[\frac{(1-2\vartheta)\tilde{u}_0^2}{8g\vartheta\tilde{\zeta}_0(1+4\kappa)}+2\mu\right]\right\}^{1/2} \leqslant r < \left[\frac{2\mu}{g\vartheta\tilde{\zeta}_0(1+\kappa)}\right]^{1/2} \tag{47}$$

The most restrictive of Ineqs. (45)–(47) and Ineq. (37) are going to be used for the experiments.

4. NUMERICAL EXPERIMENTS

The method developed in Section 3.2 was tested on the problem introduced by Beji and Battjes [7] using $L_0 = 0$ m, $L_1 = 24$ m, $T = 2$ s, $H = 0.02$ m, $h_0 = 0.4$ m and the bathymetry shown in Figure 1.

First, the method was applied for $\vartheta = 0.5$ with $\Delta x = \frac{1}{20}$ m, $\Delta t = \frac{1}{150}$ s and the surface elevation obtained for the interval $[L_0, L_1]$. Results were obtained for all stations. In each time step one prediction-correction was performed.

To investigate the effect of the parameter ϑ at the numerical solution of systems (3a), (3b) the interval [0, 1] was discretized into 20 subintervals each of width $\Delta\vartheta = 0.05$ and the method was applied for $t \in [0, 30]$ for each value ϑ. From the surface elevations only those which were in agreement with the expected solution from the experimental data [7] were obtained. From the runs it was found that this restriction was satisfied, when $\vartheta \in [0.4, 0.6]$. Then, in order to establish more precisely the behaviour of the method for the various values of ϑ, the interval [0.4, 0.6] was discretized to subintervals, each of width $\Delta\vartheta = 0.01$ and the method was applied again for $t \in [0, 30]$ for each value ϑ. After examining the resulting surface elevation in each of the stations 1–7, when $\vartheta \in [0.4, 0.6]$, no spurious oscillations were observed (see also Figures 2 and 3).

In order to evaluate the results, the solution for the various values of ϑ was compared to the solution obtained by MIKE 21 BW [15], developed by DHI Software. The set-up of the DHI model

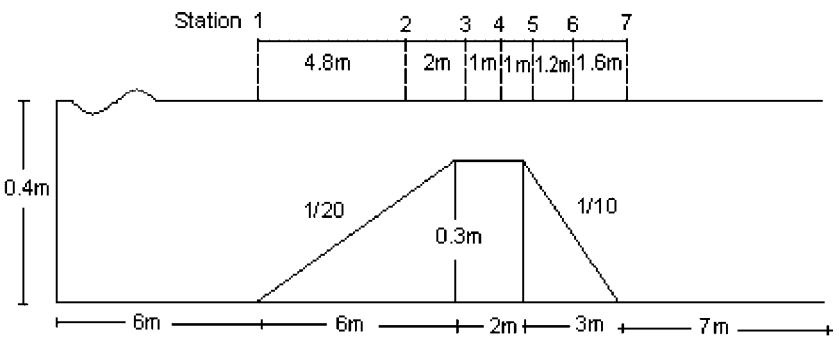

Figure 1. The bathymetry used for the experiments. The stations (st) 1–7 are the same to those used by Beji and Battjes [7].

DOI: 10.1002/fld

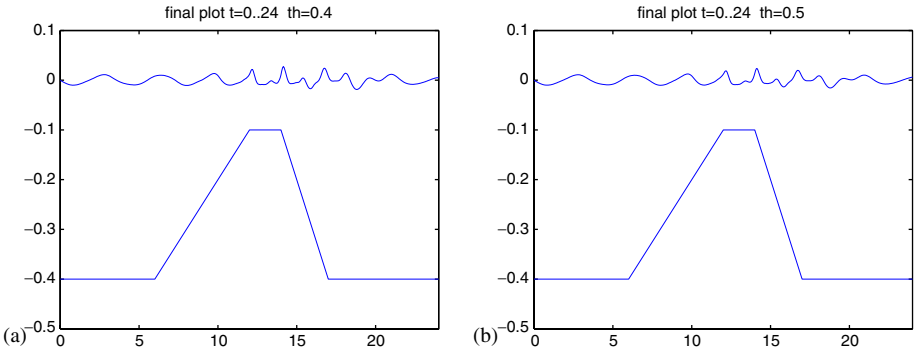

Figure 2. The curve shows the surface elevation when: (a) $\vartheta = 0.40$; and (b) $\vartheta = 0.5$.

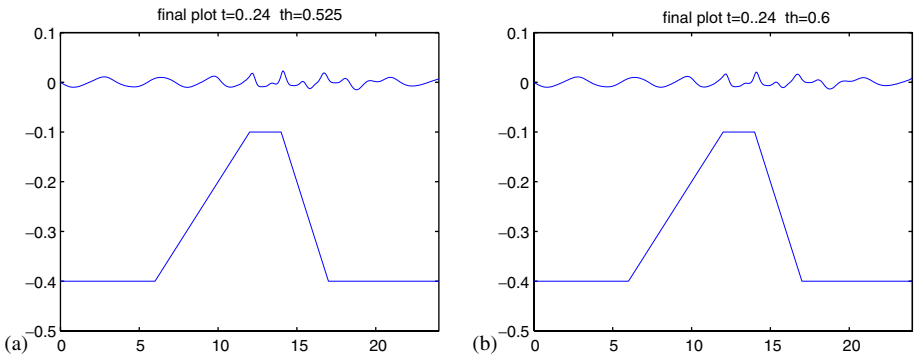

Figure 3. The curve shows the surface elevation when: (a) $\vartheta = 0.525$; (b) and $\vartheta = 0.6$.

is described as follows: a time step equal to $T/200 = 0.01$ s and a spatial step equal to $1/20 = 0.05$ m were used corresponding with a maximum Courant number equal to 0.4. The duration of the simulation was 5000 time steps or 50 s, where the first 500 time steps were considered as the warm-up period of the model (the period where the forcing functions—boundary conditions—are gradually built up to their prescribed value). The flux densities and the surface slopes, which were obtained by a wave generator of first-order Stokes waves with the characteristics of the Beji–Battjes set-up, were given to the model as source conditions, while a sponge layer of 100 points (5 m) was used 1.5 m before the source to absorb the wave energy propagation out of the model domain and 3 m after the end of the obstacle to absorb incoming waves in the computational area.

MIKE 21 BW converges to a periodic solution after 20 s for the specific configuration at stations 5, 6 and 7. In Figures 4–7 we present the resulting surface elevation of our numerical method (thin line) compared to the solution we get from MIKE (thick line) at each of the stations 2–7 for the values of $\vartheta = 0.4$, 0.45, 0.5, 0.525 and $\vartheta = 0.6$. For $\vartheta = 0.5$ the method coincides with the method presented by Beji and Battjes [7].

The MIKE 21 BW solution is considered as a reference solution, so we calculated the maximum absolute difference between our solution and the solution given by MIKE 21 BW for the various

DOI: 10.1002/fld

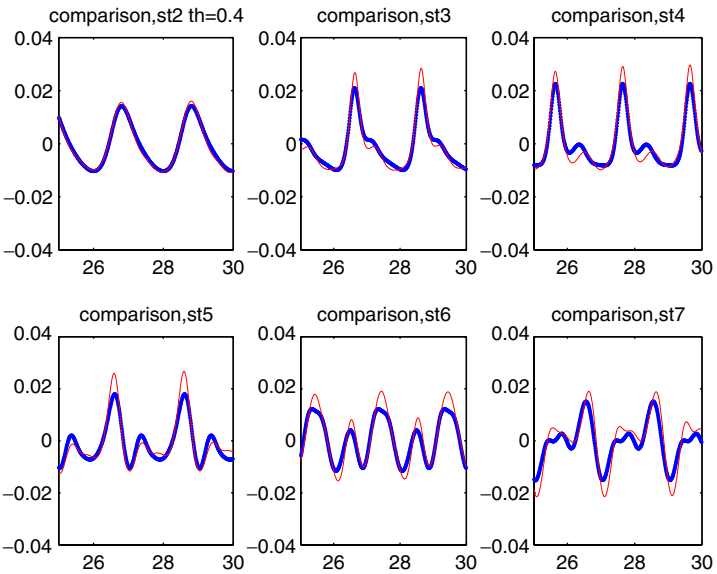

Figure 4. The curves show the surface elevation at $t \in [25, 30]$ for stations 2–7 when $\vartheta = 0.40$.

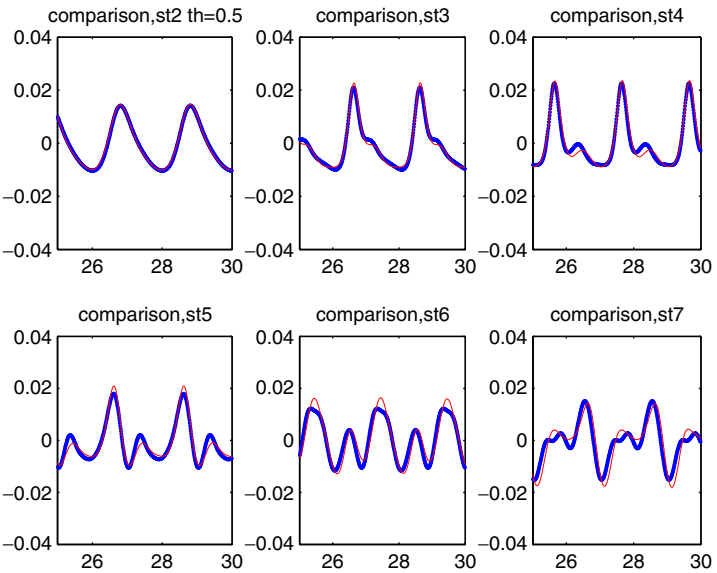

Figure 5. The curves show the surface elevation at $t \in [25, 30]$ for stations 2–7 when $\vartheta = 0.5$.

values of ϑ in each of the stations 2–7 for the time period $t \in [25, 30]$. As the two implementations have different stepsize the 'error' was measured at the common points of the discetization. The values observed for $\vartheta = 0.4$, 0.45, 0.5, 0.525 and $\vartheta = 0.6$ are presented in Table I and Figure 8.

DOI: 10.1002/fld

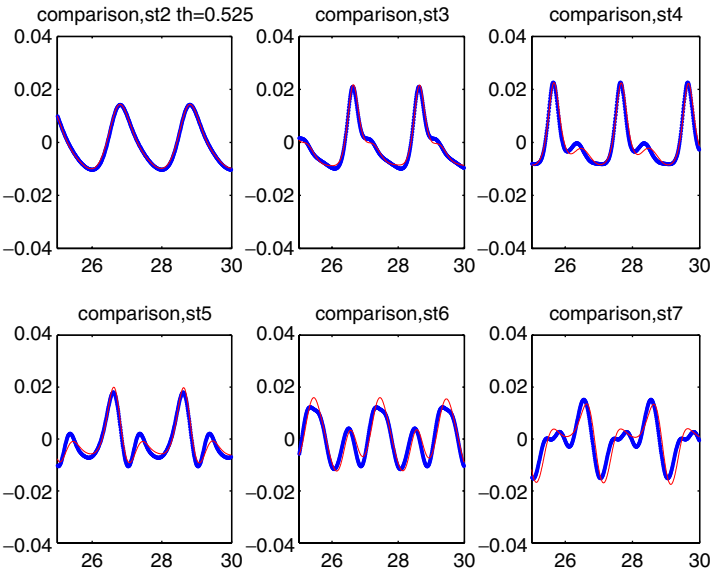

Figure 6. The curves show the surface elevation at $t \in [25, 30]$ for stations 2–7 when $\vartheta = 0.525$.

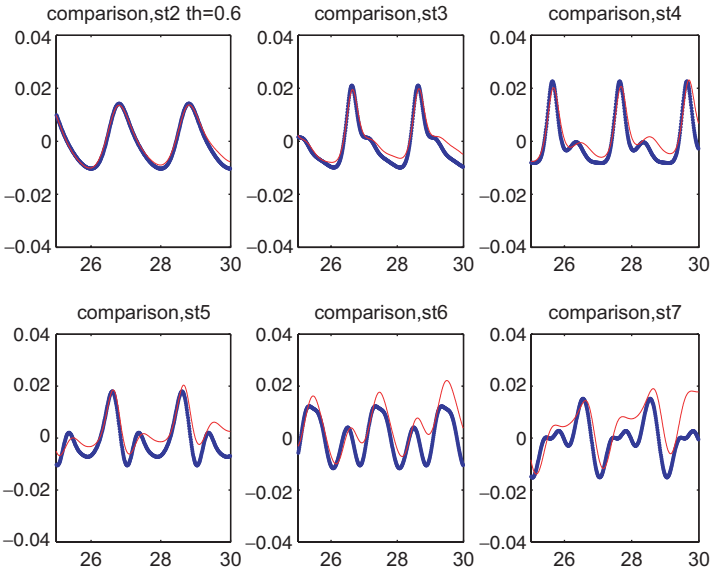

Figure 7. The curves show the surface elevation at $t \in [25, 30]$ for stations 2–7 when $\vartheta = 0.6$.

The sofar results led us to focus our choice for the best value of ϑ on the interval $[0.475, 0.525]$. So, another qualitative criterion for the evaluation of our method was added. For the various values of ϑ the invariant of motion corresponding to the conservation of mass

$$I_1 = \int_{-\infty}^{+\infty} \zeta(x, t)\, \mathrm{d}x \tag{48}$$

DOI: 10.1002/fld

Table I. The absolute value of error compared to the MIKE solution in stations 2–7 for various ϑ.

ϑ	$\vartheta=0.4$	$\vartheta=0.45$	$\vartheta=0.5$	$\vartheta=0.525$	$\vartheta=0.55$	$\vartheta=0.6$
Station 2	0.0020	0.0014	0.0013	0.0014	0.0015	0.0031
Station 3	0.0076	0.0048	0.0027	0.0023	0.0023	0.0050
Station 4	0.0071	0.0044	0.0037	0.0038	0.0043	0.0109
Station 5	0.0347	0.0317	0.0290	0.0279	0.0271	0.0291
Station 6	0.0075	0.0062	0.0049	0.0049	0.0059	0.0145
Station 7	0.0089	0.0076	0.0075	0.0076	0.0074	0.0180

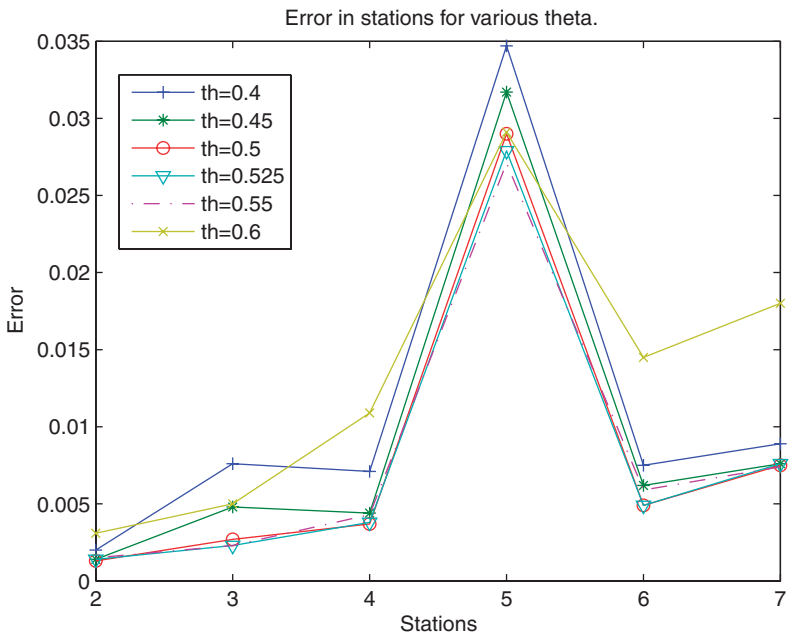

Figure 8. The absolute error for various values of ϑ in stations 2–7.

was estimated (see analogous invariant in Reference [16, p. 173]). This quantity is expected to be zero. The improper integral was estimated in an interval of x for which the solution is expected to conserve the mass. As the numerical solutions for different values of ϑ are not identical we have chosen slightly different upper and lower bounds for the various values of ϑ. Then using the composite trapezoidal rule integral (48) gives the results shown in Table II for the various values of ϑ in three time instants in the interval $t \in [25, 30]$. The overall numerical tests led to the choice of 0.525 as the most proper value for the parameter ϑ.

5. CONCLUSIONS

A parametric finite-difference scheme based on the idea of searching the *best* position between the known time level $t = n\ell$ and the unknown one $t = (n+1)\ell$ was presented in this paper for

DOI: 10.1002/fld

Table II. The absolute value of invariant for various ϑ in three time instants.

ϑ	$t=25$	$t=27$	$t=30$
0.4	0.044	0.0398	0.4190
0.425	0.0562	0.0026	0.285
0.450	0.0604	0.0306	0.1741
0.475	0.0579	0.0055	0.0850
0.50	0.0354	0.0085	0.0115
0.525	0.0140	0.00082	0.0276
0.550	0.0413	0.0451	0.0607
0.575	0.1650	0.2843	0.7132
0.60	0.1025	0.4228	0.68

the numerical solution of the one-dimensional Boussinesq-type set of equations. This position was determined with a properly introduced parameter ϑ with $\vartheta \in [0, 1]$. The method, which could be considered as a generalization of the known from the bibliography Crank-Nickolson method ($\vartheta = 0.5$), was applied successfully to the one-dimensional Boussinesq-type set of equations as those were introduced by Peregrine [2] and the experiments proved that this investigation is not non-realistic, but a fact, which gives applicable results. The numerical results compared to the corresponding ones given by the MIKE 21 BW [15] developed by DHI Software, are encouraging and specific points for improvement and optimization of the method come out from the comparisons. Consideration of different bathymetries, initial and boundary conditions could further reveal the usefulness of the proposed method.

The authors have already applied this method using different bathymetries, a work which is under preparation and it is going to be submitted for publishing soon.

ACKNOWLEDGEMENTS

This research was co-funded 75% by E.E. and 25% by the Greek Government under the framework of the Education and Initial Vocational Training Program—Archimedes, Technological Educational Institution (T.E.I.) Athens project '*Computational Methods for Applied Technological Problems*'.

The authors would like to thank Dr K. Belibassakis, Shipbuilding Department, T.E.I. Athens for the fruitful discussions during the revision of this paper.

REFERENCES

1. Berkhoff JCW. Computation of combined refraction–diffraction. In *Proceedings of 13th Coastal Engineering Conference*, vol. 1. ASCE: Vancouver, 1972; 471–490.
2. Peregrine DM. Long waves on a beach. *Journal of Fluid Mechanics* 1967; **27**(4):815–827.
3. Abbott MB, Petersen HM, Skovgaard O. On the numerical modeling of short waves in shallow water. *Journal of Hydraulic Research* 1978; **16**(3):173–203.
4. Abbott MB, McCowan AD, Warren IR. Accuracy of short wave numerical models. *Journal of Hydraulic Engineering* 1984; **110**(10):1287–1301.
5. Madsen PA, Murray R, Sørensen OR. A new form of the Boussinesq equations with improved linear dispersion characteristics (Part 1). *Coastal Engineering* 1991; **15**(4):371–388.
6. Madsen PA, Sørensen OR. A new form of the Boussinesq equations with improved linear dispersion characteristics. Part 2: a slowly-varying bathymetry. *Coastal Engineering* 1992; **18**(1):183–204.
7. Beji S, Battjes JA. Numerical simulation of nonlinear wave propagation over a bar. *Coastal Engineering* 1994; **23**:1–16.

DOI: 10.1002/fld

8. Wei G, Kirby T. Time-dependent numerical code for extended Boussinesq equations. *Journal of Waterway Port Coastal and Ocean Engineering* (ASCE) 1995; **121**(5):251–261.
9. Beji S, Nadaoka K. Formal derivation and numerical modelling of the improved Boussinesq equations for varying depth. *Ocean Engineering* 1996; **23**:691–704.
10. Madsen PA, Schäffer HA. A review of Boussinesq-type equations for surface gravity waves. In *Advances in Coastal and Ocean Engineering*, vol. 5, Liu PL-F (ed.). World Scientific: Singapore, 1999; 1–95.
11. Kirby JT. Boussinesq models and applications to nearshore wave propagation, surf zone processes and wave-induced currents. In *Advances in Coastal Engineering*, Lakhan C (ed.). Elsevier: Amsterdam, 2003.
12. Bratsos AG. A parametric scheme for the numerical solution of the Boussinesq equation. *Korean Journal of Computational and Applied Mathematics* 2001; **8**(1):45–57.
13. Courant R, Friedrichs H, Lewy. Uber die partiellen Differenzen-Greichungen der mathematischen Physik. *Mathematische Annalen* 1928; **100**:32–74.
14. Twizell EH. *Computational Methods for Partial Differential Equations*. Ellis Horwood Limited: England, 1984.
15. DHI Software, MIKE 21 BW, User Guide. In *MIKE 21*, *Wave Modelling*, *User Guide*. 2002; 271–392.
16. Hamdi S, Enright WH, Ouellet Y, Schiesser WE. Exact solutions of extended Boussinesq equations. *Numerical Algorithms* 2004; **37**:165–175.

DOI: 10.1002/fld